

Selective Integration of Waste-Derived Glass Nanopowders in Structural Wall Concrete: Improving Thermal Efficiency and Elasto-Mechanical Properties for Sustainable Construction

Abdelmoutalib Benfrid^{1*}, Mohammed Chatbi², Zouaoui R. Harrat¹, Mohamed Bachir Bouiadjra^{1,3}

¹ Laboratoire des Structures et Matériaux Avancés dans le Génie Civil et Travaux Publics, Djillali Liabes University, 22000 Sidi Bel-Abbes, P.O.B. 89, Algeria

² Department of Public Works, Mouloud Mammeri University of Tizi-Ouzou, 15000 Tizi Ouzou, Algeria

³ Thematic Agency for Research in Science and Technology (ATRST), 16004 El Harrach, P.O.B. 62, Algeria

* Corresponding author, e-mail: abdelmoutalib.benfrid@dl.univ-sba.dz

Received: 18 February 2025, Accepted: 08 July 2025, Published online: 14 July 2025

Abstract

Concrete, as a primary construction material, faces significant environmental and performance challenges, including high carbon emissions and limited thermal comfort, particularly in structural applications. This study investigates the integration of waste-derived glass nanopowder (GNP) as a sustainable additive to enhance the thermal and mechanical performance of eco-concrete. The research aims to optimize thermal comfort and structural efficiency for wall applications while promoting environmental sustainability. Using analytical homogenization models, the elasto-thermo-mechanical behavior of nano-reinforced concrete (RC) is evaluated. The Maxwell-Eucken model is employed to assess thermal conductivity, while the Luo model determines the elastic properties, accounting for the three-dimensional behavior of wall structures. The results indicate that incorporating a 30% volume fraction of GNP enhances thermal conductivity by nearly 15%, increases thermal resistance by 25%, and significantly reduces thermal expansion and the thermal transmittance coefficient (U_{hom}) by 30% and 25%, respectively. Additionally, the elastic properties are shown to adjust proportionally to the nanopowder content, ensuring compatibility with structural demands. These findings underline the potential of GNP as an efficient and sustainable additive for advanced structural applications, particularly in energy-efficient wall systems, contributing to the advancement of eco-friendly civil engineering practices.

Keywords

eco-concrete, glass nanopowder (GNP), thermo-elastic behavior, sustainable construction materials, thermal conductivity, energy-efficient wall systems

1 Introduction

Concrete is the most widely used construction material globally due to its strength, durability, and versatility [1, 2]. It forms the backbone of infrastructure, including buildings, bridges, roads, and other essential structures [3–5]. However, traditional concrete production is associated with several significant challenges, most notably its high environmental impact [6]. The cement industry, a key ingredient in concrete, is one of the largest contributors to global carbon dioxide (CO₂) emissions, accounting for approximately 7–8% of the total emissions worldwide [7]. In addition to its environmental footprint, concrete often exhibits limited thermal comfort, particularly in structural applications like walls, where heat retention or dissipation can affect energy efficiency and

indoor climate control [8]. As climate change and energy conservation become growing concerns, there is an urgent need to address these issues by enhancing concrete's performance, sustainability, and thermal efficiency.

Furthermore, the growing demand for stronger and more functional materials in construction calls for innovative solutions to enhance both the mechanical strength and thermal comfort of concrete [9, 10]. One promising solution is the integration of waste-derived glass nanopowder (GNP) into concrete mixtures [11, 12]. As a byproduct of glass recycling, GNP provides a sustainable way to improve the properties of eco-concrete [13]. Its incorporation can potentially enhance both thermal conductivity and mechanical strength, improving the durability and

overall performance of concrete [14]. GNPs unique characteristics, such as its high surface area and fine particle size, make it an ideal candidate for reinforcing concrete, particularly in structural applications like walls, where thermal comfort and mechanical performance are essential [15]. This study explores the potential of waste-derived GNP as a nano-reinforcement in concrete, with the aim of optimizing its thermal and mechanical properties for use in structural panels.

The potential of waste-derived GNP in concrete mixtures has been extensively explored in experimental research. For instance, Radhi et al. [16], investigated the use of industrial and construction waste, specifically powdered glass from waste bottles and ceramic tile waste, in reactive powder concrete (RPC). By determining the optimal ceramic-to-glass ratio through pozzolanic activity tests, they incorporated these materials as partial replacements for silica (SiO_2) fume at levels ranging from 5% to 25%. The results demonstrated significant improvements in mechanical strength at a 15% replacement level, while higher substitution levels resulted in slightly increased water absorption. This study highlights the potential of repurposing waste materials to enhance RPC properties, contributing to more sustainable construction practices. Similarly, Jalalinejad et al. [17], investigated the mechanical and durability properties of sustainable self-compacting concrete by partially substituting cement with waste glass powder at varying levels (0–30% in 7.5% increments) and incorporating 10% micro- SiO_2 as a constant additive. They assessed key performance parameters, including workability, compressive, tensile, and bending strengths, as well as surface and capillary water absorption, and freeze/thaw resistance. Their findings revealed that glass powder improved the fluidity and fresh concrete properties. However, a slight reduction in mechanical performance was observed at the highest substitution level of 30%, highlighting the importance of finding an optimal balance in sustainable mix designs. This study underscores the need to carefully optimize the proportion of GNP to achieve the best balance of sustainability and performance in concrete mixtures. Abdelli et al. [18], further expands on the use of industrial waste in concrete, specifically focusing on the combined use of glass and plastic waste. The research examined the effects of these waste materials on workability, chloride penetration, carbonation resistance, and compressive strength. The study found that the incorporation of glass and plastic waste enhanced chloride penetration resistance by 20.5% over

time. While glass powder increased carbonation depth, plastic fibers helped reduce it, demonstrating a complementary effect when combining these waste materials. This study highlights the potential of utilizing industrial waste to not only improve concrete's mechanical and durability properties but also to promote environmental sustainability in construction.

Moreover, several other experimental studies have supported the beneficial use of glass powders in concrete mixtures, contributing to improved mechanical and thermal performance. Research by Zeybek et al. [19], Elaqla and Rustom [20], Madandoust and Ghavidel [21], Amin et al. [22], and Jiang et al. [23], has demonstrated that glass powders enhance concrete's resistance to mechanical stresses such as buckling and bending, as well as its ability to withstand thermal exposures and chemical attacks. These findings further confirm the advantages of incorporating waste-derived GNP into concrete, for both improving its mechanical properties and increasing its durability under various environmental and load conditions.

In contrast to the extensive experimental studies on the use of GNP in concrete, there remains a noticeable lack of analytical investigations addressing the thermo-mechanical behavior of such structures. Few studies have utilized analytical tools to accurately describe and predict the behavior of concrete structures reinforced with GNP. One notable example is the work by Benfrid et al. [24], which presented a comprehensive thermomechanical analysis of concrete incorporating glass powder as an additive. The researchers employed the efficient Eshelby's model to determine the composite properties, taking into account the spherical shape of the glass powder particles. Additionally, the study utilized deformation plate theory to theoretically simulate reinforced concrete (RC) panels under various conditions. Their findings highlighted the challenges of integrating glass powder into concrete for thermomechanical applications, suggesting that alternative approaches are necessary to further optimize its effectiveness in such scenarios.

The critical need to improve the mechanical performance and resilience of concrete has become even more apparent in the aftermath of recent devastating seismic events, such as the 2023 Kahramanmaraş earthquakes in Türkiye. These twin earthquakes (moment magnitudes of 7.7 and 7.6) caused massive structural failures, resulting in over 50,000 casualties and the collapse of hundreds of thousands of RC buildings – many of which failed due to poor material quality, inadequate seismic detailing, or outdated

design standards [25]. Field investigations in the most affected provinces, including Hatay, Kahramanmaraş, and Adıyaman, revealed that soft-story mechanisms, short columns, and insufficient reinforcement were key contributors to structural failure, even in relatively recent constructions [26]. Further assessments showed that, despite updated seismic codes, the actual ground motions far exceeded design expectations, exposing the vulnerabilities of conventional concrete under extreme loading [27]. Moreover, structural weaknesses such as low-strength concrete, poor workmanship, and substandard reinforcement detailing significantly worsened the level of damage [28]. These tragic outcomes highlight the urgent necessity for developing advanced concrete materials with improved mechanical strength, durability, and energy dissipation capacity – particularly in seismic zones. In this context, the integration of nano-reinforcements such as waste-derived GNP presents a promising strategy to not only enhance mechanical and thermal performance but also to contribute to safer and more sustainable construction practices.

In alignment with the need for analytical investigations, several studies have employed homogenization models to derive the thermo-mechanical properties of nano-composite concrete structures. Harrat et al. [29], utilized Eshelby's homogenization model to evaluate the effects of incorporating ferric oxide (Fe_2O_3) nanoparticles into the concrete matrix, providing valuable results into their influence on composite properties. Similarly, Chatbi et al. [30], applied the Voigt homogenization model to simulate the impact of SiO_2 nano-additives on concrete performance, explicitly accounting for the agglomeration effect of nanoparticles. Furthermore, Dine Elhennani et al. [31] analyzed the mechanical performance of concrete reinforced with various nanoparticles, including SiO_2 , titanium dioxide (TiO_2), and zirconium dioxide (ZrO_2), using advanced analytical tools. These studies collectively underscore the significance of analytical approaches, demonstrating their pertinence and reliability in yielding valid results for understanding and optimizing the behavior of nano-RC structures.

This study aims to analytically investigate the thermo-mechanical properties of eco-concrete panels reinforced with waste-derived GNP, focusing on two main aspects: thermal performance and elasto-mechanical behavior. The novelty of this work lies in the integration of analytical homogenization techniques to simultaneously assess and optimize both thermal and mechanical characteristics of sustainable nano-RC – an approach still limited in the existing literature.

The first stage of the study addresses the thermal behavior of the material. Through the homogenization of thermal conductivity (λ), key thermal performance indicators are derived, including the thermal resistance (R), heat transfer coefficient (U), and heat flux (ϕ). These parameters are evaluated using the Maxwell–Eucken model [32], a widely accepted analytical framework for estimating thermal behavior in multiphase composites. This model enables a predictive understanding of how GNP inclusion influences the thermal efficiency of concrete panels, especially in building envelope applications where temperature regulation is critical.

The second stage focuses on the mechanical behavior of the composite. Using a 3D two-phase homogenization model, where the concrete matrix and the GNP phase are treated separately, we derive the effective elastic moduli (E_x , E_y , E_z), Poisson's ratios (ν_{xy} , ν_{xz} , ν_{yz}), Coulomb shear modulus (G), and compressibility modulus (K). This approach – based on Voigt [33], Reuss [34], and Voigt–Reuss [35] averaging schemes – allows for a more realistic prediction of the material's directional mechanical response. Unlike traditional isotropic assumptions, this model captures the potential anisotropic behavior introduced by the nano-inclusions, which is essential for accurately evaluating composite performance under practical loading conditions.

Taken together, the key contributions of this work are:

1. the dual analytical modeling of both thermal and mechanical properties in a unified framework;
2. the use of a 3D two-phase homogenization model to reflect anisotropic mechanical effects;
3. the promotion of a sustainable and efficient concrete design by incorporating recycled GNP to enhance energy performance and reduce environmental impact.

2 Analytical framework for evaluating thermo-mechanical properties

The analysis follows a two-phase homogenization process, considering specific hypotheses and assumptions that govern the behavior of the composite material:

1. *Phase I, "homogeneous concrete mixture"*: initially, the concrete matrix is assumed to be homogeneous and isotropic, representing the mono-phasic state of traditional concrete without any reinforcement. This serves as the baseline for evaluating the influence of the GNP inclusions.
2. *Phase II, "bi-phasic composite material"*: upon the partial incorporation of GNP as a reinforcement material, the mixture transitions into a bi-phasic

composite material. The volume percentage (vt%) of GNP reinforcement varies from 0% (pure concrete) to a maximum of 30%, allowing for an investigation of its effects at different inclusion levels.

In terms of physical assumption, the analyzed model adopts the following considerations:

- *"Spherical shape of inclusions"*: for simplicity and consistency, the GNP inclusions are assumed to have a uniform spherical shape. This hypothesis ensures analytical tractability and allows the study to focus on the effects of volume fraction and material properties. It is noted, however, that changes in the inclusion shape could alter the composite's mechanical response, particularly influencing the Poisson's ratio and elastic properties.
- *"Random distribution of inclusions"*: the GNP particles are considered to be randomly distributed throughout the concrete matrix, with no agglomeration. This ensures that the inclusions are uniformly dispersed and separated within the matrix, mimicking real-world scenarios while simplifying the homogenization procedure.

Fig. 1 illustrates the homogenization procedures and provides a visual representation of these hypotheses. It demonstrates the transition from a mono-phasic to

a bi-phasic composite, the assumed spherical geometry of the GNP inclusions, and their random, non-agglomerated distribution within the concrete matrix.

2.1 Thermal homogenization using the Maxwell–Eucken model

The Maxwell–Eucken homogenization model is a widely used theoretical approach to estimate the effective thermal conductivity of two-phase composite materials. It is particularly applicable to systems where one phase is dispersed as small spherical inclusions (GNP) within a continuous matrix (concrete), such as particles embedded in a solid medium.

This model is most effective in predicting the thermal behavior of composites with a low volume fraction of inclusions (vt%), assuming the inclusions are isotropic. The framework provides an analytical formula for the composite's effective thermal conductivity (λ_{hom}) based on the thermal conductivities of the matrix (λ_c) and the inclusion (λ_{Gp}), as well as the volume fraction of the inclusions (v_{Gp}) [32]:

$$\lambda_{hom} = \lambda_c \left\{ \frac{2\lambda_c + \lambda_{Gp}}{-2(\lambda_c - \lambda_{Gp})v_{Gp}} \right\} \left\{ \frac{2\lambda_c + \lambda_{Gp}}{+2(\lambda_c - \lambda_{Gp})v_{Gp}} \right\}^{-1}. \quad (1)$$

The model assumes steady-state heat conduction and neglects interfacial thermal resistance (thermal reflection), which simplifies its application but limits its accuracy for

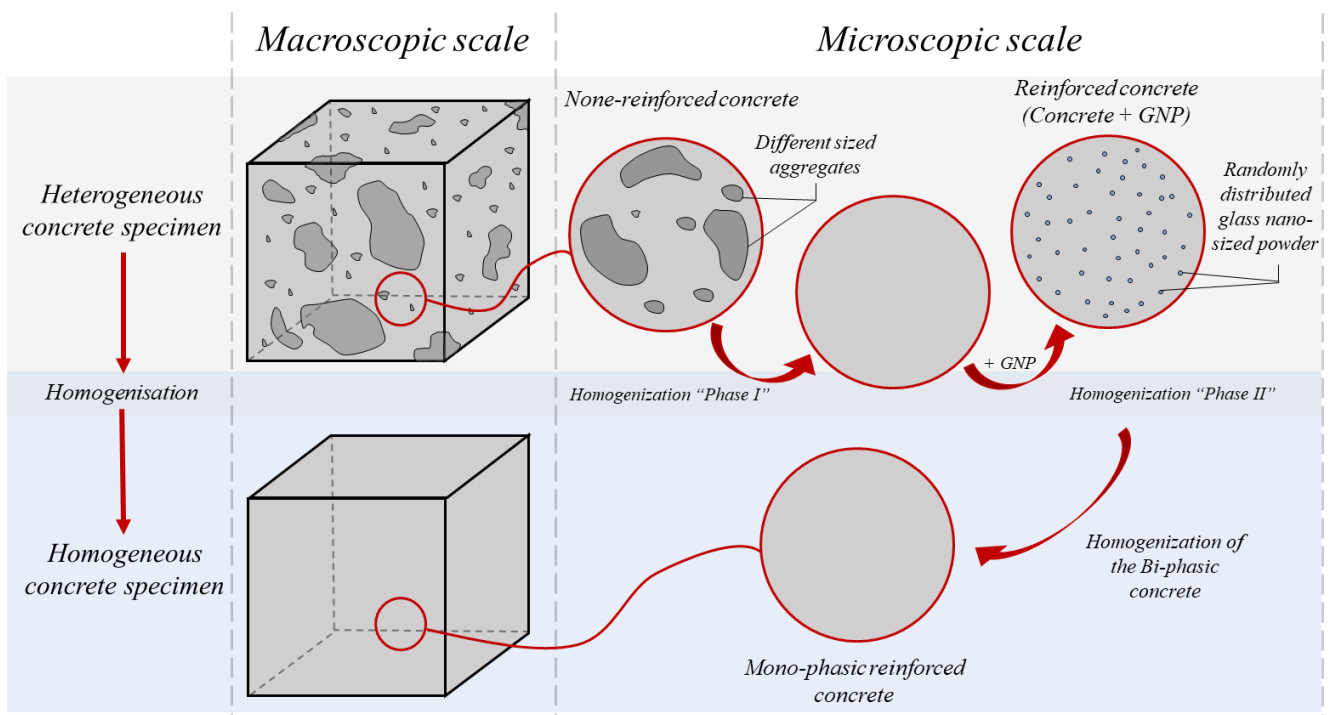


Fig. 1 Homogenization process of a concrete matrix infused with GNP, illustrating macro- and microscale interactions

materials with significant interfacial effects. It also presumes isotropic thermal properties and spherical geometry for the inclusions, as illustrated in Fig. 2.

For the representative elementary volume (REV) considered in this analysis, the volume fraction of the additives V_{Gp} is defined in relation to the volume fraction of the matrix domain V_c . This relationship is mathematically expressed in Eq. (2):

$$V_{Gp} = 1 - V_c. \quad (2)$$

To analyze the effect of GNP content on the thermal expansion of the concrete matrix, Eq. (3) accounts for the interaction between thermal expansion of the concrete matrix (α_c) and the GNP inclusions (α_{Gp}). The effective thermal expansion (α_{hom}) coefficient for the composite is expressed in Eq. (3):

$$\alpha_{hom} = V_c \alpha_c + V_{Gp} \alpha_{Gp}. \quad (3)$$

The thermal resistance (R_{hom}) of the nano-RC is then defined in Eq. (4) as the ratio of the wall thickness (e_p) to its thermal conductivity. It is measured in square meters per Celsius per Watt ($m^2 \times ^\circ C/W$), providing an indicator of the material's ability to resist heat transfer.

$$R_{hom} = e_p \lambda_{hom}^{-1} \quad (4)$$

Additionally, the thermal transmittance coefficient (denoted as U_{hom}) quantifies the amount of heat transferred through a panel (wall) and is expressed in Eq. (5):

$$U_{hom} = R_{hom}^{-1}. \quad (5)$$

Thermal flux (ϕ_{hom}) represents the amount of heat transferred through a building's wall per unit area, providing a fundamental measure of heat flow in thermal performance analysis, measured in Watt per square meter (W/m^2) and is expressed in Eq. (6):

$$\phi_{hom} = U_{hom} S_p \{T_{int} - T_{ext}\}, \quad (6)$$

where S_p is the surface area of the wall, calculated as the product of the width and height of the wall in square meters (m^2), while interior temperature (T_{int}) and exterior temperature (T_{ext}) represent the interior and exterior temperatures of the wall structure, respectively, measured in degrees Celsius ($^\circ C$).

By estimating the λ_{hom} , R_{hom} and U_{hom} of a concrete wall infused with GNPs, its heat transfer performance can be quantified, giving an idea of its thermal efficiency and potential for improving energy conservation in construction applications.

2.2 Elasto-mechanical homogenization using the Reuss–Voigt–Luo model

In Section 2.2, we apply an advanced homogenization model introduced by Luo [36], designed to estimate the effective elastic properties of a concrete matrix infused with GNP in three dimensions (x , y , z). This model accounts for the Poisson ratio effect, which is crucial for accurately characterizing the behavior of bi-phasic composites. According to Luo [36], the three elastic moduli (E_x , E_y , E_z) (GPa) can be expressed for the bi-phasic composite in Eq. (7):

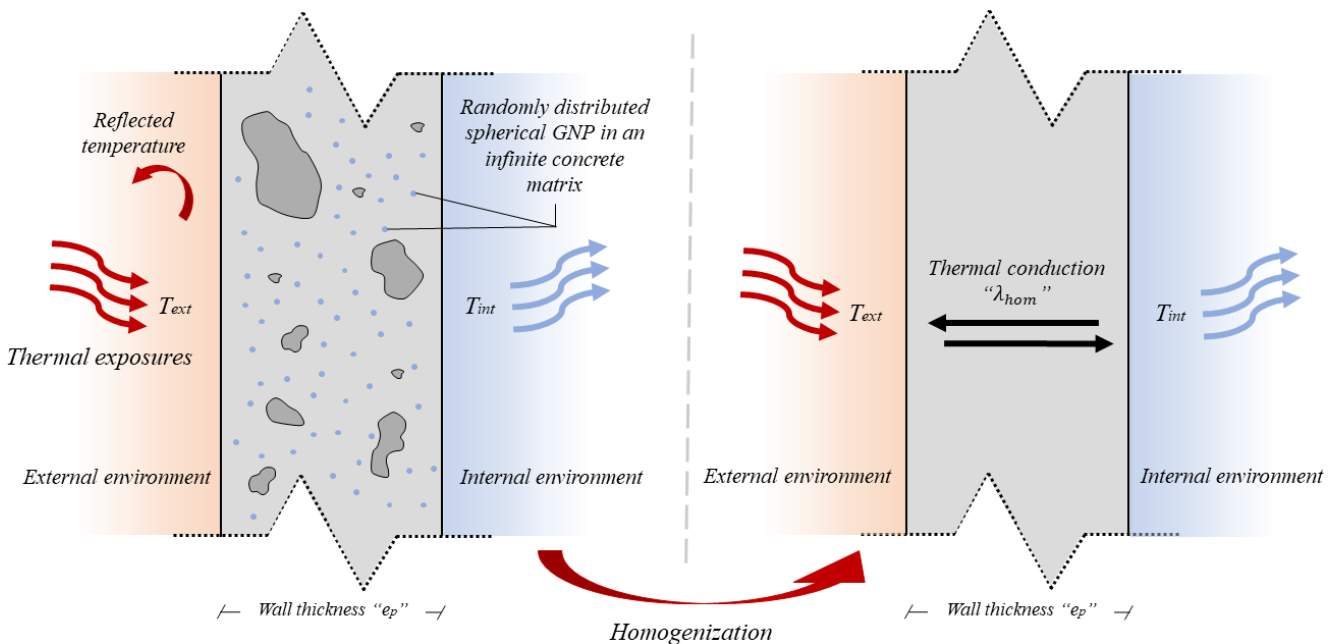


Fig. 2 Thermal conductivity across the thickness (e_p) of a concrete wall structure infused with GNP, pre- and post-homogenization

$$\begin{aligned}
 E_{hom}^x &= E_{hom}^y \\
 &= \frac{\left\{ \begin{matrix} V_c(1-\nu_{Gp})E_c \\ +V_{Gp}(1-\nu_c)E_{Gp} \end{matrix} \right\} \left\{ \begin{matrix} V_c(1+\nu_{Gp})E_c \\ +V_{Gp}(1+\nu_c)E_{Gp} \end{matrix} \right\}}{\left\{ V_c(1-\nu_{Gp}^2)E_c + V_{Gp}(1-\nu_c^2)E_{Gp} \right\}} \\
 E_{hom}^z &= \frac{E_c E_{Gp} [V_c(1-\nu_{Gp})E_c + V_{Gp}(1-\nu_c)E_{Gp}]}{\left\{ \begin{matrix} E_c E_{Gp} [V_c^2(1-\nu_{Gp}) + V_{Gp}^2(1-\nu_c)] \\ +V_{Gp}V_c \left[\begin{matrix} (1+\nu_{Gp})(1-2\nu_{Gp})E_c^2 \\ +4\nu_{Gp}\nu_c E_c E_{Gp} \\ +(1+\nu_c)(1-2\nu_c)E_{Gp}^2 \end{matrix} \right] \end{matrix} \right\}}. \quad (7)
 \end{aligned}$$

This model accounts for the Poisson's ratio effect, which plays a critical role in the regulation of the elastic properties of composite materials. Unlike the conventional Voigt and Reuss formulas, which do not consider the Poisson effect and are therefore inaccurate, this improved model incorporates the Poisson effect by deriving a set of new formulas based on the governing equations of elasticity. The three Poisson's ratios are expressed as in Eq. (8):

$$\begin{aligned}
 \nu_{hom}^{xy} &= \frac{\left\{ \begin{matrix} V_c(1-\nu_{Gp})\nu_c \\ +V_{Gp}(1-\nu_c)\nu_{Gp} \end{matrix} \right\} \left\{ \begin{matrix} V_c(1+\nu_{Gp})E_c \\ +V_{Gp}(1+\nu_c)E_{Gp} \end{matrix} \right\}}{\left\{ V_c(1-\nu_{Gp}^2)E_c + V_{Gp}(1-\nu_c^2)E_{Gp} \right\}} \\
 \nu_{hom}^{xz} &= \frac{\left\{ \begin{matrix} V_c(1+\nu_{Gp}^2)E_c\nu_c + V_{Gp}(1+\nu_c^2)E_{Gp}\nu_{Gp} \end{matrix} \right\}}{\left\{ V_c(1-\nu_{Gp}^2)E_c + V_{Gp}(1-\nu_c^2)E_{Gp} \right\}} \\
 \nu_{hom}^{zx} &= \nu_{hom}^{zy} \\
 &= \frac{E_c E_{Gp} [V_c(1-\nu_{Gp})\nu_c + V_{Gp}(1-\nu_c)\nu_{Gp}]}{\left\{ \begin{matrix} E_c E_{Gp} [V_c^2(1-\nu_{Gp}) + V_{Gp}^2(1-\nu_c)] \\ +V_{Gp}V_c \left[\begin{matrix} (1+\nu_{Gp})(1-2\nu_{Gp})E_c^2 \\ +4\nu_{Gp}\nu_c E_c E_{Gp} \\ +(1+\nu_c)(1-2\nu_c)E_{Gp}^2 \end{matrix} \right] \end{matrix} \right\}}. \quad (8)
 \end{aligned}$$

where (E_c, ν_c) and (E_{Gp}, ν_{Gp}) represent the elastic moduli and Poisson's ratios of concrete and GNP, respectively.

In addition to elastic moduli and Poisson's ratios, calculating the G (GPa) and K (GPa⁻¹) is crucial for a comprehensive understanding of the mechanical behavior of nano-RC. Matos et al. [13] provide a clear definition of the G and K . The corresponding expressions are as follows:

$$\begin{aligned}
 G_{hom}^x &= E_{hom}^x [2(1+\nu_{hom}^{xy})]^{-1} \\
 G_{hom}^y &= E_{hom}^y [2(1+\nu_{hom}^{zy})]^{-1}, \quad (9)
 \end{aligned}$$

and:

$$\begin{aligned}
 K_{hom}^x &= E_{hom}^x [3(1-2\nu_{hom}^{xy})]^{-1} \\
 K_{hom}^y &= E_{hom}^y [3(1-2\nu_{hom}^{zy})]^{-1}, \quad (10)
 \end{aligned}$$

3 Thermo-elastic properties of constituent materials

This study analytically simulates the thermo-elastic behavior of a two-phase composite material, consisting of a concrete matrix reinforced with GNPs. In our analysis, we consider two types of GNPs: SiO₂ GNP and aluminosilicate (Al-SiO₂) GNP. These two types were selected for their distinct mechanical and thermal properties, which provide a diverse range of parameters for the composite material.

3.1 Concrete matrix

The concrete matrix serves as the base material in this study, characterized by its fundamental elastic and thermal properties. Given that the analysis employs an analytical modeling approach rather than experimental methods, the mechanical behavior of the concrete is represented through simplified key parameters. These include the elastic modulus ($E_c = 20$ GPa), which defines the material's stiffness and resistance to deformation under applied stress; the Poisson's ratio ($\nu_c = 0.3$), which describes the relationship between lateral and longitudinal strains under uniaxial loading; and the thermal conductivity coefficient ($\lambda_c = 1.75 \text{ W} \times \text{m}^{-1} \times ^\circ\text{C}^{-1}$), which reflects the material's ability to conduct heat.

This simplified representation ensures that the analytical framework is both effective and efficient in assessing the behavior of the composite material, providing a reliable basis for the subsequent homogenization process.

3.2 Glass nanopowder (GNP)

Nano-sized glass powders are incorporated into the concrete mixture to develop a nano-composite matrix with enhanced mechanical and thermal properties. In this analysis, we consider two types of GNPs: SiO₂ GNP and Al-SiO₂ GNP. These additives are selected for their distinct elasto-mechanical and thermal properties, which are summarized in Table 1 [37].

Table 1 Thermo-elastic properties of GNPs [37]

Code name for GNP		Al-SiO ₂ GNP	SiO ₂ GNP
Elastic properties	Elastic modulus (E_{Gp}) (GPa)	81	73
	Poisson ratio (ν_{Gp})	0.291	0.16
	Thermal expansion (α_{Gp}) ($10^{-6}/^\circ\text{C}$)	4.6	0.55
Thermal properties	Thermal conductivity (λ_{Gp}) ($\text{W} \times \text{m}^{-1} \times ^\circ\text{C}^{-1}$)	1.15	1.15

The properties presented in Table 1 highlight the high stiffness and low thermal expansion of GNPs, making them ideal for improving the performance of concrete composites. SiO_2 GNP is particularly notable for its low thermal expansion and moderate stiffness, making it well suited to applications requiring dimensional stability under thermal loading. Al- SiO_2 GNP, on the other hand, offers greater stiffness and a moderate coefficient of thermal expansion, which significantly improves the mechanical strength of the composite while maintaining efficient thermal performance. By incorporating these nano-additives, the composite exhibits improved elastic behavior and thermal stability, which are essential for advanced structural wall applications. Walls are specifically addressed in this study because of their central role in the thermal regulation and structural integrity of buildings. Improving the thermo-elastic properties of walls contributes to reducing energy consumption by improving insulation and maintaining structural efficiency, aligning with sustainability objectives by minimizing the carbon footprint and optimizing the use of materials in construction.

4 Results and discussion

Section 4 presents a comprehensive analysis and discussion of the results obtained from the analytical modeling carried out to assess the thermo-elastic behavior of nano-RC. The study examines the influence of incorporating SiO_2 glass and Al- SiO_2 GNPs into the concrete matrix, focusing on their effects on the mechanical and thermal properties of the composite.

The analysis explores the impact of these nano-reinforcements on key parameters such as thermal conductivity and heat flow through the concrete matrix, demonstrating the contribution of GNPs to thermal regulation and energy efficiency. In addition, the effective elastic moduli and Poisson's ratio of the composite are examined in detail, highlighting the critical role of Poisson's ratio in influencing material stiffness and strain energy distribution within the composite. Furthermore, various geometries of wall panels are studied, with each wall having a width (a), height (b), and thickness (e_p), as depicted in Fig. 3.

4.1 Validation of homogenization models

To verify the accuracy of the Maxwell–Eucken homogenization model, given the lack of comprehensive studies on the thermal properties of concrete reinforced with high proportions of GNP up to 30% by volume, the model's reliability was validated against an established material

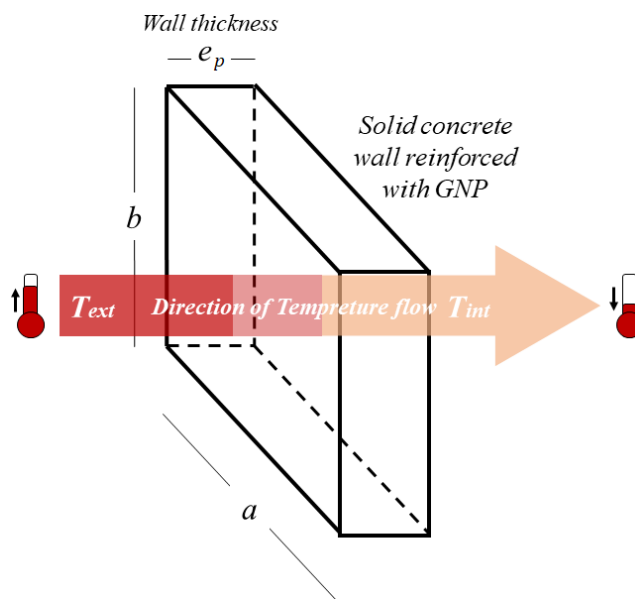


Fig. 3 Schematic representation of the wall panel geometries, with width (a), height (b), and thickness (e_p), used for analyzing the thermal and elasto-mechanical properties of GNP-infused concrete

system using experimental results from lime and hemp concrete [38]. The validation utilized data from a study that analyzed lime and hemp composites with hemp shiv inclusions up to 30% by volume. Fig. 4 illustrates the comparison between the Maxwell–Eucken model predictions and the experimental data for lime and hemp composites. As shown in Fig. 4, the close agreement between the two demonstrates the reliability of the Maxwell–Eucken homogenization model for analyzing thermal conductivity in composite materials with high-volume fractions of inclusions. This validation provides a solid basis for applying the model to the concrete matrix infused with GNP, guaranteeing the accuracy of subsequent analyses.

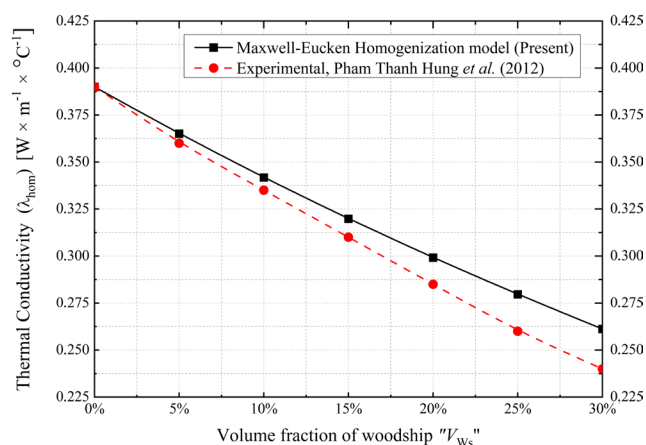


Fig. 4 Validation of the Maxwell–Eucken homogenization model: comparison of predicted and experimental thermal conductivity for lime and hemp concrete with hemp shiv inclusions up to 30% by volume

4.2 Thermal behavior of concrete walls infused with GNPs

Fig. 5 illustrates the evolution of the thermal conductivity of a concrete matrix infused with varying amounts of GNP, ranging from 0% to 30% by volume. The results in Fig. 5 clearly show a decreasing tendency in the thermal conductivity of the concrete as the volume fraction of GNPs increases. Notably, since SiO_2 GNP and Al-SiO_2 GNPs exhibit the same thermal conductivity, the behavior described in Fig. 5 applies to both types of GNP.

This observed reduction in thermal conductivity can be attributed to the inherently lower thermal conductivity of the GNPs compared to the concrete matrix. As the volume fraction of GNPs increases, the effective thermal conductivity of the composite decreases, as the GNPs disrupt the heat transfer pathways within the concrete. This thermal resistance introduced by the GNPs reduces the overall heat flow through the material.

To investigate the effect of GNP content on the thermal expansion in Celsius ($^{\circ}\text{C}^{-1}$) of the concrete matrix, Fig. 6 illustrates the relationship between the volume fraction of GNP and the thermal expansion of the concrete matrix. The results show that increasing the GNP content reduces the thermal expansion for both types of GNPs, with SiO_2 -based GNP exhibiting a greater reduction compared to Al-SiO_2 -based GNP. This greater efficiency is attributed to the inherently lower thermal expansion of SiO_2 -based GNP, which helps to reduce thermal stress in the concrete matrix. This reduction in thermal expansion contributes to the durability of wall structures by improving thermal stability, reducing the risk of cracking and improving the energy efficiency of building envelopes.

Fig. 7 illustrates the evolution of the thermal resistance of a concrete matrix infused with varying amounts of

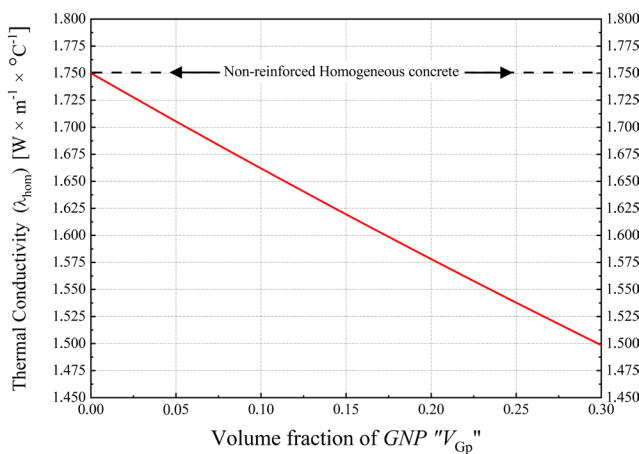


Fig. 5 Thermal conductivity (λ_{hom}) ($\text{W}/\text{m} \times ^{\circ}\text{C}$) as a function of the volume fraction of GNP, V_{Gp}

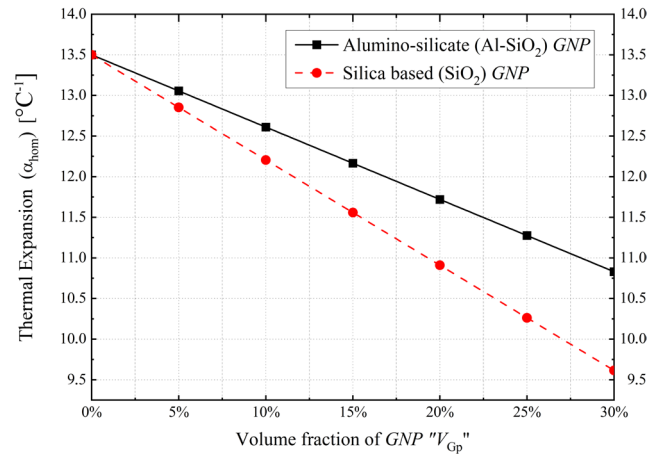


Fig. 6 Thermal expansion of the concrete matrix as a function of GNP content for Al-SiO_2 and SiO_2 based GNPs

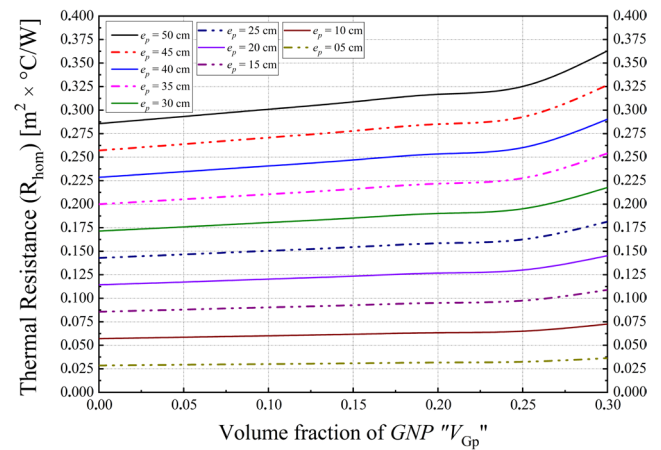


Fig. 7 Thermal resistance (R_{hom}) ($\text{m}^2 \times ^{\circ}\text{C}/\text{W}$) as a function of the volume fraction of GNP, V_{Gp}

GNPs from 0% to 30% by volume. In this analysis, the wall thickness varied from $e_p = 5$ cm to $e_p = 50$ cm to evaluate the combined effects of wall geometry and material composition on thermal resistance.

As expected, the thermal resistance increases with the volume fraction of GNPs, directly confirming the trend observed in Fig. 5 regarding the reduction in thermal conductivity. Notably, when the volume fraction of GNP reaches 25%, a pronounced increase in thermal resistance is observed, marking a higher rate of change compared to lower concentrations of GNP. This sudden trend can be attributed to the percolation threshold of nanopowders in the concrete matrix. At this stage, the GNP distribution probably forms a more effective network of thermal barriers, significantly disrupting heat transfer pathways and amplifying thermal resistance. The variation in wall thickness further highlights the importance of design considerations in optimizing thermal performance. Thicker walls combined with higher concentrations of GNP achieve substantial improvements

in thermal resistance, reinforcing the suitability of GNP-infused concrete for energy-efficient wall structures.

Fig. 8 shows the variation in U_{hom} with increasing GNP volume fractions, for different wall thicknesses. As Fig. 8 shows, the U decreases systematically as the GNP volume fraction increases, whatever the wall thickness. This behavior is consistent with the reduction in thermal conductivity observed in Figs. 6 and 7. Since the U is inversely related to the thermal resistance (R), the increase in thermal resistance due to the presence of GNPs leads to a reduction in U . Essentially, the more GNPs are incorporated into the concrete matrix, the more the material's ability to transmit heat decreases, helping to improve insulation performance.

Table 2 presents the ϕ_{hom} in Watts, as a function of the volume fraction of GNPs, for two types of panels (square and rectangular).

As shown in Table 2, the negative values of thermal flux represent energy dissipation, indicating heat loss from the interior to the exterior environment. Although not present in the current dataset, positive values would correspond to energy input or heat gain. Table 2 displays results under both summer (Sum.) conditions ($T_{int} = 18\text{ }^{\circ}\text{C}$, $T_{ext} = 43\text{ }^{\circ}\text{C}$) and winter (Win.) conditions ($T_{int} = 32\text{ }^{\circ}\text{C}$, $T_{ext} = -6\text{ }^{\circ}\text{C}$). The analysis considers three wall thicknesses: $e_p = 20\text{ cm}$, $e_p = 30\text{ cm}$, and $e_p = 50\text{ cm}$, with the volume fraction of GNP varying from 0% to 30%. The data presented in Table 2 reflect the impact of both the volume fraction of GNPs and the wall thickness on thermal flux. As the volume fraction of GNPs increases, the thermal flux decreases, aligning with previous observations that higher GNP concentrations reduce thermal conductivity and consequently limit heat transfer.

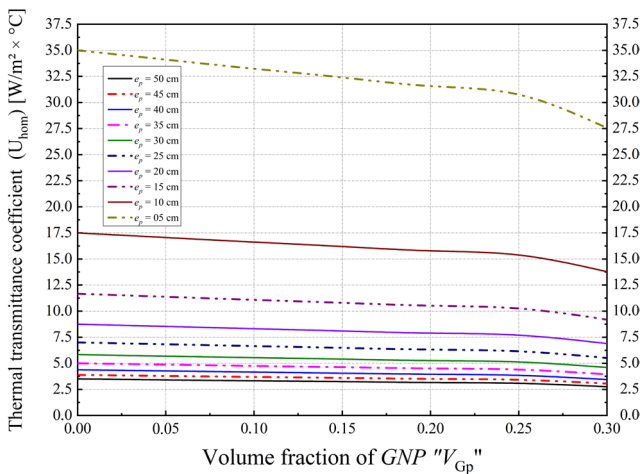


Fig. 8 The U_{hom} of a concrete matrix ($\text{W/m}^2 \times ^{\circ}\text{C}$) as a function of the volume fraction of GNP, V_{Gp}

Table 2 Thermal flux (ϕ_{hom}) (Watt) as a function of the volume fraction of GNP (V_{Gp}) for two panel types (square and rectangular) during summer (Sum.) ($T_{int} = 18\text{ }^{\circ}\text{C}$; $T_{ext} = 43\text{ }^{\circ}\text{C}$) and winter (Win.) ($T_{int} = 32\text{ }^{\circ}\text{C}$; $T_{ext} = -6\text{ }^{\circ}\text{C}$)

Square panel ($a \times b$) = (3×3) m^2						
V_{Gp}	$e_p = 50\text{ cm}$		$e_p = 30\text{ cm}$		$e_p = 20\text{ cm}$	
	Win.	Sum.	Win.	Sum.	Win.	Sum.
0%	1197	-788	1995	-1313	5985	-3938
5%	1167	-767	1944	-1279	5833	-3837
10%	1137	-748	1895	-1247	5684	-3739
15%	1108	-729	1846	-1215	5539	-3644
20%	1080	-710	1799	-1184	5398	-3551
25%	1052	-692	1753	-1153	5260	-3460
30%	942	-620	1571	-1033	4712	-3100
Rectangular panel ($a \times b$) = (3×2.5) m^2						
V_{Gp}	$e_p = 50\text{ cm}$		$e_p = 30\text{ cm}$		$e_p = 20\text{ cm}$	
	Win.	Sum.	Win.	Sum.	Win.	Sum.
0%	998	-656	1663	-1094	4988	-3281
5%	972	-640	1620	-1066	4860	-3198
10%	947	-623	1579	-1039	4737	-3116
15%	923	-607	1539	-1012	4616	-3037
20%	900	-592	1499	-986	4498	-2959
25%	877	-577	1461	-961	4383	-2884
30%	785	-517	1309	-861	3926	-2583
Rectangular panel ($a \times b$) = (2×2.5) m^2						
V_{Gp}	$e_p = 50\text{ cm}$		$e_p = 30\text{ cm}$		$e_p = 20\text{ cm}$	
	Win.	Sum.	Win.	Sum.	Win.	Sum.
0%	665	-438	1108	-729	3325	-2188
5%	648	-426	1080	-711	3240	-2132
10%	632	-416	1053	-692	3158	-2077
15%	615	-405	1026	-675	3077	-2024
20%	600	-395	1000	-658	2999	-1973
25%	584	-385	974	-641	2922	-1922
30%	524	-344	872	-574	2618	-1722

Furthermore, Table 2 also illustrates how wall thickness plays a significant role in the thermal flux. Thicker walls consistently exhibit lower thermal flux values, as they offer greater thermal resistance, which reduces the amount of heat passing through the material.

4.3 Elasto-mechanical behavior of concrete walls infused with GNPs

In Section 4.3, the study focuses on analyzing the elasto-mechanical properties of concrete walls reinforced with different types of GNPs. Specifically, the investigation considers two types of GNPs: Al-SiO₂ GNP and SiO₂ GNP, with the results for each type presented in Tables 3 and 4, respectively. Table 5 compares the uncertainties between the two types of RC, based on the effective material properties derived from the analysis.

Table 3 Elasto-mechanical properties of eco-concrete incorporating Al-SiO₂ GNP

V_{GP} of Al-SiO ₂	E_{hom}^x	E_{hom}^y	E_{hom}^z	ν_{hom}^{xy}	ν_{hom}^{xz}	$\nu_{hom}^{zx} = \nu_{hom}^{zy}$	G_{hom}^x	G_{hom}^y	G_{hom}^z	K_{hom}^x	K_{hom}^y	K_{hom}^z
0%	1.093	1.093	20.000	0.015	0.300	0.300	0.530	0.341	6.250	0.375	0.910	16.667
5%	1.075	1.075	19.422	0.013	0.298	0.331	0.524	0.337	5.843	0.368	0.889	19.152
10%	1.062	1.062	19.277	0.011	0.297	0.365	0.519	0.333	5.573	0.362	0.873	23.751
15%	1.052	1.052	19.415	0.010	0.296	0.401	0.515	0.330	5.388	0.358	0.860	32.628
20%	1.044	1.044	19.763	0.009	0.295	0.438	0.512	0.328	5.265	0.355	0.851	53.530
25%	1.037	1.037	20.289	0.008	0.295	0.476	0.510	0.326	5.195	0.352	0.843	142.747
30%	1.032	1.032	20.976	0.008	0.294	0.512	0.508	0.325	5.179	0.349	0.836	280.311

Table 4 Elasto-mechanical properties of eco-concrete incorporating SiO₂ GNP

V_{GP} of SiO ₂	E_{hom}^x	E_{hom}^y	E_{hom}^z	ν_{hom}^{xy}	ν_{hom}^{xz}	$\nu_{hom}^{zx} = \nu_{hom}^{zy}$	G_{hom}^x	G_{hom}^y	G_{hom}^z	K_{hom}^x	K_{hom}^y	K_{hom}^z
0%	1.026	1.026	20.000	0.015	0.300	0.300	0.498	0.321	6.250	0.353	0.855	16.667
5%	1.022	1.022	19.617	0.013	0.277	0.324	0.498	0.329	5.954	0.350	0.765	18.550
10%	1.019	1.019	19.568	0.011	0.260	0.349	0.498	0.335	5.764	0.347	0.706	21.563
15%	1.016	1.016	19.753	0.010	0.245	0.374	0.498	0.341	5.647	0.346	0.664	26.222
20%	1.014	1.014	20.121	0.009	0.233	0.400	0.498	0.346	5.590	0.344	0.633	33.514
25%	1.012	1.012	20.649	0.008	0.223	0.424	0.498	0.350	5.587	0.343	0.609	45.230
30%	1.010	1.010	21.324	0.007	0.215	0.445	0.498	0.353	5.643	0.342	0.590	64.289

Table 5 Comparison of the elasto-mechanical properties of eco-concretes based on Al-SiO₂ GNP and SiO₂ GNP

V_{GP}	ΔE_{hom}^x	ΔE_{hom}^y	ΔE_{hom}^z	$\Delta \nu_{hom}^{xy}$	$\Delta \nu_{hom}^{xz}$	$\Delta \nu_{hom}^{zx} = \Delta \nu_{hom}^{zy}$	ΔG_{hom}^x	ΔG_{hom}^y	ΔG_{hom}^z	ΔK_{hom}^x	ΔK_{hom}^y	ΔK_{hom}^z
0%	0.066	0.066	0.000	0.000	0.000	0.000	0.032	0.021	0.000	0.023	0.055	0.000
5%	0.053	0.053	-0.195	0.000	0.021	0.007	0.026	0.008	-0.111	0.018	0.124	0.602
10%	0.043	0.043	-0.291	0.000	0.038	0.016	0.021	-0.002	-0.191	0.015	0.167	2.188
15%	0.036	0.036	-0.338	0.000	0.051	0.026	0.017	-0.011	-0.259	0.012	0.196	6.406
20%	0.030	0.030	-0.358	0.000	0.062	0.039	0.015	-0.018	-0.325	0.011	0.218	20.015
25%	0.026	0.026	-0.360	0.000	0.072	0.052	0.012	-0.023	-0.392	0.009	0.234	97.517
30%	0.022	0.022	-0.349	0.001	0.080	0.068	0.010	-0.029	-0.464	0.008	0.246	216.022

From the data presented in Tables 3 and 4, it is evident that the introduction of GNPs leads to a general trend of decreased values for the elastic moduli (E_{hom}^x , E_{hom}^y), Poisson's ratios (ν_{hom}^{xy}), shear moduli (G_{hom}^x , G_{hom}^y), and compressibility moduli (K_{hom}^x , K_{hom}^y), reflecting a reduction in the material's ability to resist deformation under stress. On the other hand, the values of the elastic modulus along the z-axis (E_{hom}^z), Poisson's ratios (ν_{hom}^{xz} , ν_{hom}^{zy}), shear moduli (G_{hom}^z), and compressibility moduli (K_{hom}^z), show an increase, indicating a greater resistance to deformation in the direction perpendicular to the plane of the wall.

From an application perspective, this behavior has significant implications for wall structures in energy-efficient buildings. By reducing the thermal conductivity, GNP-RC can act as a more effective insulator, minimizing heat transfer between the interior and exterior environments. This property is particularly advantageous for enhancing the thermal performance of building envelopes, reducing energy consumption for heating and cooling, and contributing to sustainability goals.

The ability to control and fine-tune the thermal conductivity of concrete through the incorporation of GNPs makes it a promising material for constructing walls in green buildings and other applications where thermal insulation is a critical design consideration.

5 Conclusions

This study highlights the potential of waste-derived GNP as a sustainable additive for improving the thermal and mechanical properties of eco-concrete. Incorporating up to 30% GNP by volume resulted in significant improvements in the thermal conductivity, thermal resistance, and thermal transmittance coefficient of the concrete, suggesting GNPs role in enhancing energy efficiency and thermal comfort in buildings. The research also demonstrates that the elasto-mechanical properties of GNP-infused concrete adjust proportionally to the GNP content, providing added structural benefits.

Key parameters such as the volumetric fraction of glass powder and the geometry of the concrete panels were

found to significantly influence the thermal and mechanical characteristics of eco-concretes. In particular, Al-SiO₂ and SiO₂ glass powders enhanced both the mechanical strength and thermal stability of the concrete, with the Al-SiO₂ reinforcement showing superior performance.

This research supports sustainable construction by proposing a cost-effective and environmentally responsible solution for enhancing the thermal performance of concrete wall structures. The incorporation of waste-derived GNP significantly improves thermal resistance and reduces heat transfer, contributing to lower energy consumption in buildings. This leads to decreased heating and cooling demands, thereby reducing operational energy use and associated carbon emissions. Additionally, the use of recycled glass helps minimize waste and reduces reliance on cement, further lowering the environmental impact. Overall, GNP-reinforced eco-concrete offers a promising pathway toward energy-efficient, low-carbon building

materials, fully aligned with global sustainability objectives in the construction sector.

Future research can build on the analytical framework presented in this study to explore other types of nano-reinforcements, different composite formulations, or structural configurations. In particular, further work should investigate the long-term durability, environmental performance, and scalability of GNP-RC in real-world applications. Such investigations will be essential to validate and extend the current findings, and to advance the development of sustainable, energy-efficient construction materials grounded in both experimental and analytical approaches.

Acknowledgement

The authors gratefully acknowledge the Thematic Agency for Research in Science and Technology (ATRST) in Algeria for their valuable technical support.

References

- [1] Montayev, S., Omarov, B., Ristavletov, R., Dosov, K., Montayeva, N., Dosaliev, K. "Sintering and Crystallization Intensifiers for Production of Ceramic Paving Blocks by Vibropressing Technology", *Periodica Polytechnica Civil Engineering*, 67(3), pp. 706–715, 2023.
<https://doi.org/10.3311/PPci.21818>
- [2] Mehta, P. K. "Concrete, Structure, Properties and Materials", Prentice-Hall, 1986. ISBN 0131671154
- [3] Yilmaz, S., Özmen, H. B. (eds.) "High Performance Concrete Technology and Applications", IntechOpen, 2016. ISBN 978-953-51-2651-5
<https://doi.org/10.5772/61562>
- [4] Neville, A. M. "Properties of Concrete", Pearson Education Limited, 2011. ISBN 978-0273755807
- [5] Neville, A. M. "Properties of Concrete", Longman Scientific & Technical, 1995. ISBN 0-582-23070-5
- [6] Jähren, P., Sui, T. "Concrete and Sustainability", CRC Press, 2013. ISBN 978-1-4665-9249-0
- [7] Purnell, P. "The carbon footprint of reinforced concrete", *Advances in Cement Research*, 25(6), pp. 362–368, 2013.
<https://doi.org/10.1680/adcr.13.00013>
- [8] Ghoreishi, A. "Assessment of Thermal Mass Property for Energy Efficiency and Thermal Comfort in Concrete Office Buildings", PhD dissertation, University of Illinois at Urbana-Champaign, 2015. [online] Available at: <https://www.ideals.illinois.edu/items/79523> [Accessed: 17 January 2025]
- [9] Neville, A. M., Brooks, J. J. "Concrete Technology", Longman Scientific & Technical, 1987. ISBN 0-470-20716-7
- [10] Kosmatka, S. H., Panarese, W. C., Kerkhoff, B. "Design and Control of Concrete Mixtures", Portland Cement Association, 2002. ISBN 0-89312-217-3
- [11] Onaizi, A. M., Lim, N. H. A. S., Huseien, G. F., Amran, M., Ma, C. K. "Effect of the addition of nano glass powder on the compressive strength of high volume fly ash modified concrete", *Materials Today: Proceedings*, 48, pp. 1789–1795, 2022.
<https://doi.org/10.1016/j.matpr.2021.08.347>
- [12] Huseien, G. F., Khalid, N. H. A., Mirza, J. "Nanotechnology for Smart Concrete", CRC Press, 2022. ISBN 9781003196143
<https://doi.org/10.1201/9781003196143>
- [13] Matos, A. M., Milheiro-Oliveira, P., Pimentel, M. "Eco-efficient high performance white concrete incorporating waste glass powder", *Construction and Building Materials*, 411, 134556, 2024.
<https://doi.org/10.1016/j.conbuildmat.2023.134556>
- [14] Salemi, N., Behfarnia, K., Zaree, S. A. "Effect of nanoparticles on frost durability of concrete", *Asian Journal of Civil Engineering*, 15(3), pp. 411–420, 2014.
- [15] Safi, H. U., Behsoodi, M. M., Sharifi, M. N. "A Comparative Analysis of Compressive and Flexural Strength in Concrete with Partial Cement Replacement using Waste Glass Powder", *Indonesian Journal of Material Research*, 2(1), pp. 16–22, 2024.
<https://doi.org/10.26554/ijmr.20242120>
- [16] Radhi, M. S., M. R. Abdul Rasoul, Z., Alsaad, A. J. "Mechanical Behavior of Modified Reactive Powder Concrete with Waste Materials Powder Replacement", *Periodica Polytechnica Civil Engineering*, 65(2), pp. 649–655, 2021.
<https://doi.org/10.3311/PPci.17298>
- [17] Jalalinejad, M., Hemmati, A., Mortezaei, A. "Mechanical and Durability Properties of Sustainable Self-compacting Concrete with Waste Glass Powder and Silica Fume", *Periodica Polytechnica Civil Engineering*, 67(3), pp. 785–794, 2023.
<https://doi.org/10.3311/PPci.21537>

- [18] Abdelli, H. E., Kennouche, S., de Aguiar, J. L. B., Jesus, C. "The Combined Effect of Glass and Plastic Waste on Concrete Properties: Experimental Study", *Periodica Polytechnica Civil Engineering*, 68(4), pp. 1122–1131, 2024.
<https://doi.org/10.3311/PPci.23337>
- [19] Zeybek, Ö., Özkılıç, Y. O., Karalar, M., Çelik, A. İ., Qaidi, S., Ahmad, J., Burduhos-Nergis, D. D., Burduhos-Nergis, D. P. "Influence of Replacing Cement with Waste Glass on Mechanical Properties of Concrete", *Materials*, 15(21), 7513, 2022.
<https://doi.org/10.3390/ma15217513>
- [20] Elaqla, H., Rustom, R. "Effect of using glass powder as cement replacement on rheological and mechanical properties of cement paste", *Construction and Building Materials*, 179, pp. 326–335, 2018.
<https://doi.org/10.1016/j.conbuildmat.2018.05.263>
- [21] Madandoust, R., Ghavidel, R. "Mechanical properties of concrete containing waste glass powder and rice husk ash", *Biosystems Engineering*, 116(2), pp. 113–119, 2013.
<https://doi.org/10.1016/j.biosystemseng.2013.07.006>
- [22] Amin, M., Agwa, I. S., Mashaan, N., Mahmood, S., Abd-Elrahman, M. H. "Investigation of the Physical Mechanical Properties and Durability of Sustainable Ultra-High Performance Concrete with Recycled Waste Glass", *Sustainability*, 15(4), 3085, 2023.
<https://doi.org/10.3390/su15043085>
- [23] Jiang, X., Xiao, R., Bai, Y., Huang, B., Ma, Y. "Influence of waste glass powder as a supplementary cementitious material (SCM) on physical and mechanical properties of cement paste under high temperatures", *Journal of Cleaner Production*, 340, 130778, 2022.
<https://doi.org/10.1016/j.jclepro.2022.130778>
- [24] Benfrid, A., Benbakhti, A., Harrat, Z. R., Chatbi, M., Krour, B., Bouiadja, M. B. "Thermomechanical Analysis of Glass Powder Based Eco-concrete Panels: Limitations and Performance Evaluation", *Periodica Polytechnica Civil Engineering*, 67(4), pp. 1284–1297, 2023.
<https://doi.org/10.3311/PPci.22781>
- [25] Binici, B., Yakut, A., Kadas, K., Demirel, O., Akpinar, U., Canbolat, A., Yurtseven, F., Oztaskin, O., Aktas, S., Canbay, E. "Performance of RC buildings after Kahramanmaraş Earthquakes: lessons toward performance based design", *Earthquake Engineering and Engineering Vibration*, 22(4), pp. 883–894, 2023.
<https://doi.org/10.1007/s11803-023-2206-8>
- [26] Işık, E., Avcil, F., Hadzima-Nyarko, M., İzol, R., Büyüksaraç, A., Arkan, E., Radu, D., Özcan, Z. "Seismic Performance and Failure Mechanisms of Reinforced Concrete Structures Subject to the Earthquakes in Türkiye", *Sustainability*, 16(15), 6473, 2024.
<https://doi.org/10.3390/su16156473>
- [27] Ozturk, M., Arslan, M. H., Korkmaz, H. H. "Effect on RC buildings of 6 February 2023 Turkey earthquake doublets and new doctrines for seismic design", *Engineering Failure Analysis*, 153, 107521, 2023.
<https://doi.org/10.1016/j.engfailanal.2023.107521>
- [28] Işık, E., Avcil, F., İzol, R., Büyüksaraç, A., Bilgin, H., Harirchian, E., Arkan, E. "Field Reconnaissance and Earthquake Vulnerability of the RC Buildings in Adıyaman during 2023 Türkiye Earthquakes", *Applied Sciences*, 14(7), 2860, 2024.
<https://doi.org/10.3390/app14072860>
- [29] Harrat, Z. R., Chatbi, M., Krour, B., Hadzima-Nyarko, M., Radu, D., Amziane, S., Bachir Bouiadja, M. "Modeling the Thermoelastic Bending of Ferric Oxide (Fe_2O_3) Nanoparticles-Enhanced RC Slabs", *Materials*, 16(8), 3043, 2023.
<https://doi.org/10.3390/ma16083043>
- [30] Chatbi, M., Krour, B., Benatta, M. A., Harrat, Z. R., Amziane, S., Bouiadja, M. B. "Bending analysis of nano-SiO₂ reinforced concrete slabs resting on elastic foundation", *Structural Engineering and Mechanics*, 84(5), pp. 685–697, 2022.
<https://doi.org/10.12989/sem.2022.84.5.685>
- [31] Dine Elhennani, S., Harrat, Z. R., Chatbi, M., Belbachir, A., Krour, B., Işık, E., Harirchian, E., Bouremana, M., Bachir Bouiadja, M. "Buckling and Free Vibration Analyses of Various Nanoparticle Reinforced Concrete Beams Resting on Multi-Parameter Elastic Foundations", *Materials*, 16(17), 5865, 2023.
<https://doi.org/10.3390/ma16175865>
- [32] Eucken, A. "Allgemeine Gesetzmäßigkeiten für das Wärmeleitvermögen verschiedener Stoffarten und Aggregatzustände" (General laws for the thermal conductivity of different types of materials and states of aggregation), *Forschung auf dem Gebiet des Ingenieurwesens A*, 11(1), pp. 6–20, 1940. (in German)
<https://doi.org/10.1007/BF02584103>
- [33] Voigt, W. "Ueber die Beziehung zwischen den beiden Elasticitätsconstanten isotroper Körper" (On the relationship between the two elasticity constants of isotropic bodies), *Annalen der Physik*, 274(12), pp. 573–587, 1889. (in German)
<https://doi.org/10.1002/andp.18892741206>
- [34] Voigt, W. "Lehrbuch der Kristallphysik (mit Ausschluss der Kristalloptik)" (Textbook of crystal physics (with the exclusion of crystal optics)), Vieweg+Teubner Verlag Wiesbaden, 1966. ISBN 978-3-663-15316-0 (in German)
<https://doi.org/10.1007/978-3-663-15884-4>
- [35] Reuss, A. "Berechnung der Fließgrenze Von Mischkristallen auf Grund Der Plastizitätsbedingung für Einkristalle" (Calculation of the yield point of solid solutions based on the plasticity condition for single crystals), *ZAMM - Journal of Applied Mathematics and Mechanics / Zeitschrift für Angewandte Mathematik und Mechanik*, 9(1), pp. 49–58, 1929. (in German)
<https://doi.org/10.1002/zamm.19290090104>
- [36] Luo, Y. "Improved Voigt and Reuss Formulas with the Poisson Effect", *Materials*, 15(16), 5656, 2022.
<https://doi.org/10.3390/ma15165656>
- [37] Dubiel, M., Yang, X., Schneider, R., Hofmeister, H., Schicke, K. D. "Structure and properties of nanoparticle glass composites", *Physics and Chemistry of Glasses*, 46(2), pp. 148–152, 2005.
- [38] Pham, T. H., Férec, J., Picandet, V., Tronet, P., Costa, J., Pilvin, P. "Etude expérimentale et numérique de la conductivité thermique d'un composite chaux-chanvre" (Experimental and Numerical Study of the Thermal Conductivity of a Lime-Hemp Composite), presented at XXXe Rencontres AUGC-IBPSA, Chambéry, France, June 06–08., 2012. (in French) [online] Available at: https://www.researchgate.net/publication/265728925_Etude_experimentale_et_numerique_de_la_conductivite_thermique_d%27un_composite_chaux-chanvre [Accessed: 17 January 2025]